

# The wetting behavior of NiAl and NiPtAl on polycrystalline alumina

A. Gauffier · E. Saiz · A. P. Tomsia ·  
P. Y. Hou

Received: 20 June 2007 / Accepted: 9 August 2007 / Published online: 29 August 2007  
© Springer Science+Business Media, LLC 2007

**Abstract** In order to understand the beneficial effect of Pt on the adherence of thermally grown alumina scales, sessile drop experiments were performed to study the wetting of poly-crystalline alumina by nickel–aluminum alloys with or without platinum addition ranging from 2.4 to 10 at%. Subsequent interfacial morphology was examined using atomic force microscopy. Platinum addition enhances the wettability of NiAl alloys on alumina, reduces the oxide/alloy interface energy and increases the interfacial mass transport rates.

## Introduction

Metal/oxide interfaces are involved in many technologically important systems [1, 2]. One example that is of particular interest to this work is the critical interface that forms between  $\text{Al}_2\text{O}_3$  and its underlying alloy or coating when the metal is exposed at elevated temperatures. The reason this interface is *critical* is because failure often occurs there due to poor oxide–metal adhesion. Such failure can affect the metal component that the  $\text{Al}_2\text{O}_3$  scale is supposed to protect from continued oxidation attack. Even worse, it can cause thermal barrier coatings (TBC's), which are deposited on top of the  $\text{Al}_2\text{O}_3$ -forming alloys or coatings, to spall with the alumina.

There are three well known methods for improving the alumina layer adherence: addition of a reactive element, such as Y, Hf or Zr [3], reduction of sulphur impurity in the alloy [4], and alloying with precious metals, in particular Pt [5–7]. In fact, the oxidation performance of commercial aluminide coatings has been enhanced by platinum additions during the last 30 years [8], but the mechanism of this phenomenon is still unknown. The high sulphur affinity of a reactive element may prevent sulphur segregation to the oxide/metal interface, which causes a decrease of the interfacial strength [9]. Such an effect is not expected for Pt, because the heat of formation for a reactive element sulfide is 3–5 times greater than that of Pt sulfide, and Pt sulfide is even less stable than Al sulfide [10, 11].

The goal of this study is to understand the beneficial effect of Pt on  $\text{Al}_2\text{O}_3$  scale adhesion by evaluating how Pt affects the  $\text{Al}_2\text{O}_3/\text{NiAl}$  interface. Wetting experiments of alumina by nickel–aluminium alloys and nickel–aluminium–platinum alloys with the sessile drop method [12] are used. Although usual oxidation temperatures (1,100–1,200 °C) are much lower than those at which the experiments are conducted (1,650 °C), a wetting experiment has been chosen because it is a well established probe by which to measure basic interfacial thermodynamic quantities, such as the work of adhesion [13]. Furthermore, characterization of the interface morphology, i.e., grain boundary grooving, after the wetting experiments offers insights into the interface energies and its mass transport properties [14–21].

A. Gauffier  
Ecole de Mines d'Albi-Carmaux, Campus Jarlard – route de  
Teillet, Albi, CT Cedex 09, France

E. Saiz · A. P. Tomsia · P. Y. Hou (✉)  
Materials Sciences Division, Lawrence Berkeley National  
Laboratory, Berkeley, CA 94720, USA  
e-mail: PYHou@lbl.gov

## Experimental methods

The alloys used in this study were (in at%): Ni–25Al, Ni–37Al, Ni–37Al–5Pt, Ni–37Al–10Pt, Ni–40Al, Ni–50Al,

Ni–50Al–2.4Pt, and Ni–50Al–10Pt. All alloys were made with high-purity constituent metals into  $7 \times 1.3$  mm bars. Most of them, except for the Ni–40Al and the Ni–50Al–2.4Pt, were fabricated at Ames National Laboratory into drop-cast bars by argon-arc melting; the as-cast bars were heat treated in argon for 6 h at 1,200 °C, then 48 h at 1150 °C. The Ni–50Al–2.4Pt was made at Oak Ridge National Lab by induction melting, followed by annealing at 1,300 °C for 4 h. The Ni–40Al was made at Lawrence Berkeley National Lab by arc-melting, followed by heat treatment at 1,150 °C for 15 h. Test coupons approximately 1 mm in diameter were cut from the bars, and then further cut into 2 mm<sup>3</sup> pieces for wetting studies. Polycrystalline alumina (99.999%, Showa-Denko, Japan) substrates with average grain size of approximately 20  $\mu$ m were prepared following a procedure described in detail elsewhere [15]. The alloy pieces, before the wetting experiments, were roughly grounded on 240 grit SiC to remove any surface oxide. The alloy and alumina substrates were then cleaned ultrasonically in acetone, followed by ethanol and then distilled water.

Wetting experiments were performed by melting the pieces of Ni–Al or Ni–Pt–Al alloy on polycrystalline alumina substrates in a small closed alumina crucible. Under this condition, the equilibrium oxygen partial pressure,  $p(\text{O}_2)^{\text{eq}}$ , inside the crucible is close to the phase boundary value at which the Al alloy and  $\text{Al}_2\text{O}_3$  coexist [22–24]. Tests were conducted in a vacuum furnace under  $5 \times 10^{-6}$  Torr. The heating rate was 25 °C/min up to 1,650 °C, and then the temperature was maintained for 1 h at 1,650 °C. This temperature is above the highest melting point of the alloy studied, (1,638 °C for Ni–50Al). After 1 h, the furnace power was turned off. Contact angles between each alloy and the alumina were measured using a goniometer, after cooling down. Although this may cause some changes of the contact angle from its equilibrium value at high temperature, such changes are usually small [19]. Furthermore, the purpose of this work is to determine the relative wetting behaviour of NiAl alloys with or without Pt addition, so with drop sizes and cooling conditions being the same for all samples, the values determined at room temperature should accurately indicate any effect due to the presence of Pt, even though contact angles were not determined in situ. A few tested alumina surfaces, after mechanically or chemically removing the alloy droplet, were studied using Atomic Force Microscopy (AFM) to examine the alumina grain boundary groves beneath the droplet.

## Results and discussion

Platinum additions to the  $\beta$ -NiAl alloys were found to consistently decrease the contact angle for a given Al

content by about 6% ( $4\text{--}5^\circ$ ) and the reduction is independent of the amount of Pt added, from 2.4 to 10 at% (Fig. 1, where data from refs [15, 25–27] are also included for comparison). This result suggests that platinum additions improve the wettability between the alloys and alumina, and this should improve interfacial bonding.

Metal/oxide interfaces, such as Ni/ $\text{Al}_2\text{O}_3$  are in fact ternary systems for which the oxygen activity is a fundamental variable. The Ni/ $\text{Al}_2\text{O}_3$  couple can coexist in equilibrium over a range of  $p(\text{O}_2)$ . In this compatibility range, the composition of the bulk phases can change and, due to adsorption, the surface and interfacial energies and the contact angle can vary with oxygen activity [28, 29]. If the metal/oxide coexistence field extends over a large  $p(\text{O}_2)$  range, there can be a “plateau” region in which all the interfaces are stoichiometric, and consequently the interfacial energies are independent of oxygen activity. Adsorption of oxide species when the oxygen activity approaches the high  $p(\text{O}_2)$  limit of the coexistence region, and of aluminum rich species at the low  $p(\text{O}_2)$  limit, will decrease the surface and interfacial energies and the equilibrium contact angles. Under our experimental conditions (experiments performed in a closed crucible under vacuum), the composition of the NiAl alloy fixes the activity of aluminum,  $a_{\text{Al}}$ , and when alumina is in contact with the alloy,  $a_{\text{O}}$  is also fixed ( $a_{\text{Al}}^2 a_{\text{O}}^3 = K(T)$ ). Consequently, the oxygen activity inside the closed crucible is expected to be set to the value corresponding to the equilibrium between the NiAl alloy and the alumina. The

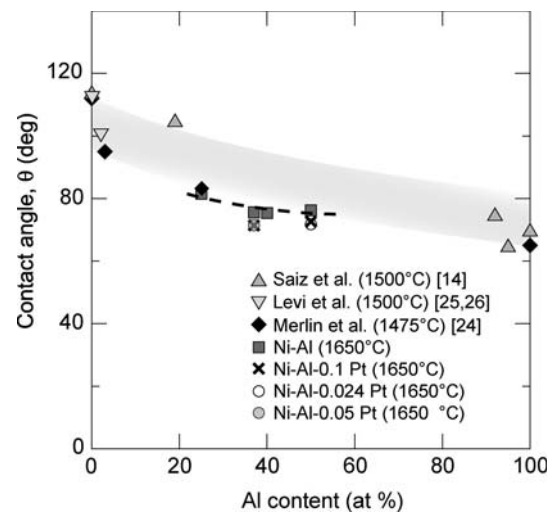


**Fig. 1** Relationship between contact angle and the aluminum concentration. The data for pure Ni is taken under conditions in which no oxygen adsorption is expected on the metal surface (either high vacuum or purified He). Since the three sets of data for Ni–xAl were performed at different temperatures, there is some degree of scattering. Nevertheless all data follows a similar trend: increasing the aluminium concentration leads to a decrease of the contact angle, and the addition of Pt consistently lowers  $\theta$  by  $4\text{--}5^\circ$

higher the content of Ni in the alloy, the lower is the aluminium activity and the higher the oxygen activity. Since the liquid has large amounts of aluminum (above 20 at%) the oxygen activity in the system is close to the low  $p(\text{O}_2)$  limit of the coexistence range and the surfaces and interfaces are aluminum rich [15, 26, 27, 30]. In this region, increasing the aluminum activity reduces the contact angle (Fig. 1). Since the addition of platinum has been shown to decrease Al activity [31], higher contact angles for the Ni–Pt–Al system could be expected. However, our results show a decrease of the contact angle, indicating that the effect of Pt on wetting is beyond that of decreasing the Al activity.

According to the Young's equation  $\gamma_{\text{iF}} = \gamma_{\text{ox}} - \gamma_{\text{m}} \cos \theta$ , where  $\gamma_{\text{ox}}$ ,  $\gamma_{\text{iF}}$  and  $\gamma_{\text{m}}$  are, respectively, the oxide surface, the metal/oxide interface, and the metal surface energies, and  $\theta$  is the contact angle. Although formations of triple line ridges at the edge of liquid droplets can limit the validity of this equation [32, 33], such complication does not apply here because the ridges are small compared with the radius of the drop. In this limit, the contact angle tends towards a value close to that given by the Young's equation [32]. The surface energies of the alloys,  $\gamma_{\text{m}}$ 's, were not determined in this study, because  $\gamma_{\text{m}}$  can only be accurately measured using the sessile drop method when the liquid poorly wets the solid, i.e.,  $\theta$  being  $>90^\circ$ . However, a recent study by first principles calculation [34] showed that 6 at% Pt addition in  $\beta$ -NiAl noticeably increases the alloy surface energy from 1.80 to 2.44 J/m<sup>2</sup>. Therefore, since Pt reduces  $\theta$ , and increases  $\gamma_{\text{m}}$ , it should decrease the metal/oxide interface energy. In terms of interface strength, the decrease of  $\gamma_{\text{iF}}$  and the increase of  $\gamma_{\text{m}}$  caused by Pt addition should increase the work of adhesion, as  $W_{\text{ad}} = \gamma_{\text{ox}} + \gamma_{\text{m}} - \gamma_{\text{iF}}$  [34].

Figure 2 shows that the surface of alumina in the vicinity of the alloy drop is strongly faceted whereas its interface with the drop is smooth. This suggests that the solid/liquid interface is more isotropic than the solid/gas interface. The measured dihedral angle,  $\Phi$ , for the alumina surface is  $\sim 148^\circ$ , independently of the composition of the drop (Table 1), and the width of the grooves ranges between 1.8 and 2.0  $\mu\text{m}$  after 1 h of annealing. Grain

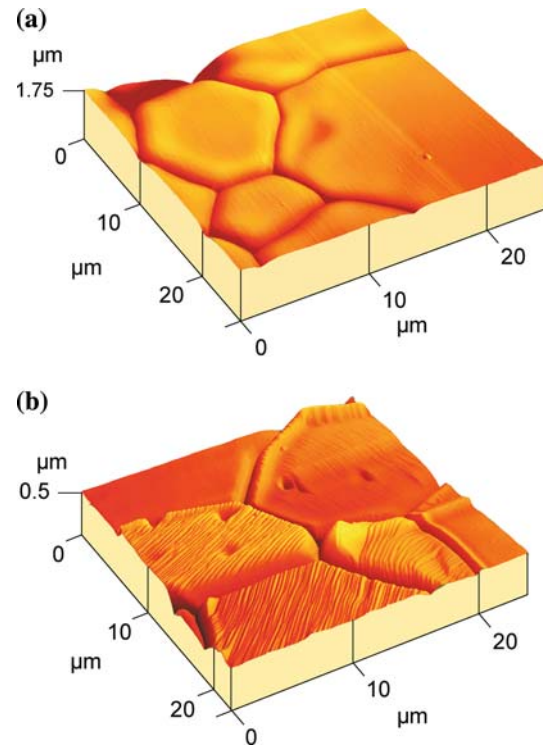


**Fig. 2** Three dimensional AFM scans (constant force mode) of an  $\text{Al}_2\text{O}_3$  area (a) under and (b) outside the Ni–37Al–5Pt droplet

boundary grooves at the solid/liquid interfaces are noticeably wider and deeper than those at the solid surfaces. The addition of Pt decreases the measured dihedral angle and increases the depth and width of the grain boundary grooves at the solid/liquid interface (Table 1); the decrease of dihedral angle may be greater with higher concentrations of Pt in the alloy. The grain boundary grooves under the Pt-containing alloys were always more symmetrically shaped than those under the alloy without platinum, in that the humps on either side of the groove were more even. This could mean that the  $\text{Al}_2\text{O}_3/\text{Ni-Pt-Al}$  interfaces are more isotropic than the  $\text{Al}_2\text{O}_3/\text{Ni-Al}$  interfaces.

A decrease in dihedral angle could be the consequence of a reduced interfacial energy. By definition, the dihedral angle,  $\Phi$ , is the equilibrium angle that forms when a boundary intersects an interface where  $\gamma_{\text{gb}} = 2\gamma_{\text{iF}} \cos(\Phi/2)$ ;

**Table 1** Average dihedral angle measured by AFM traces from grain boundaries of  $\text{Al}_2\text{O}_3$  after wetting experiments

Alloy	Inside the drop			Outside the drop		
	Dihedral angle ( $^\circ$ )	Width ( $\mu\text{m}$ )	Depth (nm)	Dihedral angle, $\Phi$	Width ( $\mu\text{m}$ )	Depth (nm)
Ni–37Al	147.2 $\pm$ 4.1	3.2 $\pm$ 0.5	261 $\pm$ 47	150.6 $\pm$ 5.8	2.0 $\pm$ 0.4	146 $\pm$ 51
Ni–37Al–5Pt	140.2 $\pm$ 6.2	3.4 $\pm$ 0.4	286 $\pm$ 38	146.4 $\pm$ 4.0	1.8 $\pm$ 0.4	146 $\pm$ 28
Ni–37Al–10Pt	136.9 $\pm$ 5.7	3.5 $\pm$ 0.3	337 $\pm$ 46	147.2 $\pm$ 7.5	1.9 $\pm$ 0.3	159 $\pm$ 52

$\gamma_{gb}$  in our case is the grain boundary energy of the alumina. It has been shown for metal/alumina systems that dihedral angles for grooves narrower than 5  $\mu\text{m}$  can be overestimated from AFM measurements, because the tip can not always penetrate close enough to the root of the groove [15]. Therefore, the true dihedral angles should be larger than those values reported in Table 1. Nevertheless, since the grain boundary widths did not vary much between the alloys, the data can be trusted in comparison, whereby the effect of Pt is consistently shown to lower the dihedral angle.

The decrease of the interfacial energy  $\gamma_{iF}$  found with NiPtAl may explain why sulphur impurity does not segregate to the interfaces between thermally grown  $\text{Al}_2\text{O}_3$  and Pt-containing Ni–Al alloys [35]. Since the driving force for segregation is directly related to the interface or surface energy [36], a lower energy would result in less segregation. Although this is a reasonable explanation, it should be noted that Pt also reduces sulphur segregation to alloy surfaces [35, 37], while by first principles calculation [34], Pt increases the alloy surface energy. Therefore, the reason why Pt reduces S segregation to NiPtAl surfaces and prevents segregation at  $\text{Al}_2\text{O}_3/\text{NiPtAl}$  interfaces [35] is still not resolved. It is possible that Pt reduces the S activity in the alloy, not by forming a sulphide like the reactive elements, but perhaps by increasing the S solubility.

The grain boundary groove profiles at the solid–liquid and solid–vapor interfaces (Fig. 3), show humps on either side of the roots which indicate that the kinetics are limited by diffusion, rather than the alumina dissolution and precipitation process. Diffusion occurs through two paths: the volume of the liquid or solid phase, or through the surface. Transport of the  $\text{Al}_2\text{O}_3$  involves diffusion of both Al and O ions or atoms. Although each species could move independently along either path, the dissolution and deposition

must involve stoichiometric  $\text{Al}_2\text{O}_3$ , such that the movement of the slowest specie through the fastest path will control the kinetics of groove evolution. Grooving is much faster under the drop, where the fastest path is volume diffusion through the liquid [15, 18]. The measured groove widths can be used to estimate the volume diffusivity  $xD_v$ , where  $x$  is the molar solubility and  $D_v$  is the volume diffusion coefficient of the controlling species [15, 19–21]. The volume diffusivities determined from our grooving measurements are of the order of  $10^{-13} \text{ m}^2 \text{ s}$ , which are close to those observed in similar systems [15]. If the diffusion coefficient in the liquid is  $D_v \approx 10^{-9} \text{ m}^2 \text{ s}^{-1}$  (a typical value for liquid metals) [38], the estimated solubility of the slow, controlling species in the liquid droplet would be  $x \sim 10^{-4}$ , and it is similar to those measured for Ni/ $\text{Al}_2\text{O}_3$  interfaces [15]. Since the liquids contain larger quantities of Al as compared to O, oxygen rich species should be controlling the kinetics of grain boundary grooving in these systems. Pt is known to reduce Al activity [31] and consequently to increase oxygen activity; in this way it will increase the controlling diffusivity resulting in faster grooving. This is consistent with the experimental observation of wider and deeper interfacial grain boundary grooves when the liquid contains platinum (Table 1).

At the surface of alumina the grooving kinetics are controlled by surface diffusion. The calculated surface diffusivity for the slowest species are of the order or  $10^{-20} \text{ m}^3 \text{ s}^{-1}$ , which is slightly larger than the rates typically reported for alumina at these temperatures [15, 19–21, 39]. However, the diffusivities determined in this work were measured under low oxygen activities, and likely correspond to non-stoichiometric surfaces, while most of the published data have been measured for much higher oxygen activities.

## Conclusions

Wetting experiments using the sessile drop method were performed with different nickel–aluminum alloys (with or without platinum additions) on poly-crystalline alumina substrates. Platinum was found to improve the wettability, to reduce the metal/ceramic interfacial energy and to increase the work of adhesion between  $\text{Al}_2\text{O}_3$  and Ni–Al alloys. Platinum additions also increased the mass transport rates at the interface between the liquid Ni–Al alloys and alumina, and decreased the anisotropy of the solid/liquid interfaces.

**Acknowledgements** The authors thank Ms. Kunie Priimak for assistance with some of the experimental work, and Prof. Brian Gleeson of Iowa State University and Dr. Bruce Pint of Oak Ridge National Lab for supplying alloys. This work was supported by the Director, Office of Science, Office of Basic Energy Sciences,

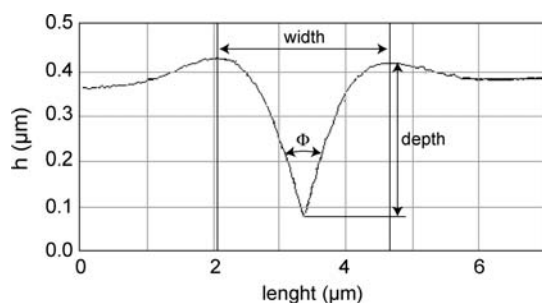


**Fig. 3** AFM line trace across an alumina grain boundary inside the wetting droplet showing measurements of boundary dihedral angle, width and depth. The dihedral angle is the angle between two tangents drawn on the grain surfaces connected with the grain boundary at the groove; the width is defined as the distance between the two highest points on each side of the boundary, and the depth is the distance from these highest points to the lowest point of the groove

Materials Sciences and Engineering Division, of the U.S. Department of Energy under Contract No. DE-AC02-05CH11231.

## References

- Rèuhle M (1990) Metal-ceramic interfaces: proceedings of an international workshop, Santa Barbara, California, USA, 16–18 January 1989. Pergamon, Oxford, New York
- Moya JS, Lopez-Esteban S, Pecharrómán C (2007) *Prog Mat Sci* 52:1017
- Whittle DP, Stringer J (1980) *Phil Trans Roy Soc Lond A* 295:309
- Smialek JL (1991) *Metall Trans A* 22:739
- Felten EJ (1976) *Oxid Met* 10:23
- Haynes JA, More KL, Pint BA, Wright IG, Cooley K, Zhang Y (2001) *Mater Sci Forum* 369–372:679
- Zhang Y, Haynes JA, Lee WY, Wright IG, Pint BA, Cooley KM, Liaw PK (2001) *Metall Mater Trans A* 32: 1727
- Lowrie R, Boone DH (1977) *Thin Solid Films* 45:491
- Funkenbusch AW, Smeggil JG, Bornstein NS (1985) *Metall Trans A* 16:1164
- Sigler DR (1989) *Oxid Met* 32:337
- CRC handbook of chemistry and physics (1990) CRC Press, Boca Raton, FL
- Sobczak N, Singh M, Asthana R (2005) *Curr Opin Solid St M* 9:241
- Eustathopoulos N, Sobczak N, Passerone A, Nogi K (2005) *J Mater Sci* 40:2271
- Nikolopoulos P (1985) *J Mater Sci* 20:3993
- Saiz E, Cannon RM, Tomsia AP (1999) *Acta Mater* 47:4209
- Kingery WD (1954) *J Am Ceram Soc* 37:42
- Mclean M, Hondros ED (1971) *J Mater Sci* 6:19
- Feingold AH, Li CY (1968) *Acta Metallurgica* 16:1101
- Mullins WW, Shewmon PG (1959) *Acta Metallurgica* 7:163
- Mullins WW (1960) *Trans Am Inst Mining Metall Eng* 218:354
- Mullins WW (1957) *J Appl Phys* 28:333
- Ricci E, Passerone A (1993) *Mat Sci Eng A* 161:31
- Ricci E, Arato E, Passerone A, Costa P (2005) *Adv Colloid Interface Sci* 117:15
- Saiz E, Tomsia AP, Sukanuma K (2003) *J Eur Ceram Soc* 23:2787
- Merlin V, Eustathopoulos N (1995) *J Mater Sci* 30:3619
- Levi G, Clarke DR, Kaplan WD (2004) *Interface Sci* 12:73
- Levi G, Scheu C, Kaplan WD (2001) *Interface Sci* 9:213
- Saiz E, Tomsia AP, Cannon RM (1998) In: Tomsia AP, Glaeser AM (eds) *Ceramic microstructures. Control at the atomic level*. Plenum Press, New York, p 65
- Chatain D, Chabert F, Ghetta V, Fouletier J (1994) *J Am Ceram Soc* 77:197
- Saiz E, Cannon RM, Tomsia AP (2000) *Acta Mater* 48:4449
- Hayashi S, Wang W, Sordelet DJ, Gleeson B (2005) *Metall Mater Trans A* 36A:1769
- Saiz E, Tomsia AP, Cannon RM (1998) *Acta Mater* 46:2349
- Saiz E, Tomsia AP, Cannon RM (2001) *Scripta Mater* 44:159
- Yu R, Hou PY (2007) *Appl Phys Lett* 91:011907
- Hou PY, McCarty KF (2006) *Scripta Mater* 54:937
- de Plessis J (1990) *Diffusion and defect data-solid state phenomena*. Sci-Tech Publish, Liechtenstein
- Cadoret Y, Bacos MP, Josso P, Maurice V, Marcus P, Zanna S (2004) *Mater Sci Forum* 461–464:247
- Smithells CJ, Brandes EA (1976) *Metals reference book*. Butterworths, London
- Dynys JM, Coble RL, Coblenz WS, Cannon RM (1980) In: Kuczynski GC (ed) *Sintering Processes*. Plenum Press, New York, p 391